Performance assessment of an optimal load control algorithm for providing contingency service

Jonathan Brooks*, Rodrigo D. Trevizan†, Prabir Barooah*, and Arturo S. Bretas†
*Department of Mechanical and Aerospace Engineering
University of Florida, Gainesville, Florida
†Department of Electrical and Computer Engineering
University of Florida, Gainesville, Florida

***Abstract*—In prior work, the Distributed Gradient Projection (DGP) algorithm was proposed to allow loads or load aggregators to provide contingency service to the grid using local frequency measurements. The DGP algorithm was shown to perform well in linear simulations. The goal of this work is to evaluate the performance of the DGP algorithm in more realistic scenarios and its robustness to issues of practical implementation, such as time delay, model mismatch, measurement noise, and stochastic disturbance. Simulation results from the IEEE 39-bus system indicate that the DGP algorithm performs well in mitigating the effects of contingencies and that it is robust to issues of practical implementation.**

I. Introduction

An important class of ancillary services required to maintain stability of the power grid is contingency services, which refers to actions taken to correct demand-supply imbalance after a contingency event such as a generator or transmission line trip [1]. Typically, generators are tasked with providing this service. An alternative that has drawn increasing attention is the use of smart loads as contingency reserves.

One question that arises in the control of smart loads for providing grid support is how to apportion the control effort (i.e., change in demand) among various loads in a fair manner. If the loads are of the same type, consumers' quality of service (QoS) can be maintained by ensuring that some signal that measures QoS stays within predetermined bounds. For instance, if the loads are air conditioners, then as long as indoor temperature variation of each unit is within a small predetermined band, the question of appropriate distribution of control effort among the loads can be avoided. However, when loads are heterogenous, such a uniform measure of QoS may be lacking. In fact, it is envisioned that in the future grid, aggregators will play the role of a middleman between the grid operators and consumers [2]–[4]. An aggregator may have a large number of heterogenous loads within its service sector, such as multiple commercial-building HVAC systems, many residential water heaters and pool pumps, etc. Moreover, the capacity of each aggregator may be not only different, but itself elastic—with more capacity available at a higher "cost"—rather than a fixed inflexible capacity that is known ahead of time. In such a scenario, it is more appropriate to distribute the effort among the aggregators by minimizing the total cost involved in executing the control action. Since this cost may not be strictly monetary but may vary depending on the type of consumers involved and their perception of service obtained etc. we refer to this cost as a *disutility*. The disutility is assumed to be a function of the demand variation from the nominal demand.

In our prior work [5], the Distributed Gradient Projection (DGP) algorithm was proposed to compute control actions for a group of agents (loads or load aggregators) with flexible demand by solving an optimization problem: minimize total disutility among all the agents subject to the constraint that the total demand-supply imbalance is made 0. The change in demand to meet the constraint provides the contingency service, while the minimization is meant to provide an optimal distribution of effort among heterogenous agents. The algorithm is distributed: agents use locally obtained frequency measurements and inter-agent communication to compute their control actions. Finally, the algorithm preserves privacy: only gradient information is sent to other loads—not demand or disutility. Simulations indicated the algorithm is successful in mitigating frequency deviations following a contingency, and it was also proven that the distributed decisions computed by the algorithm converge to the central optima. Both the simulation-based evaluations and the theoretical results in [6] were obtained under a number of simplifying assumptions.

In this paper, (1) we assess the performance of the DGP algorithm under more realistic situations (than what was done in [6]), and (2) we examine the robustness of the DGP algorithm to various uncertainties and errors that are inevitable when deployed in practice. We do this by testing the algorithm on the IEEE 39-bus test system under a variety of conditions, such as effects of measurement noise, communication delay, and distributed renewable generation. Of particular interest is the DGP algorithm's robustness to model mismatch. In the DGP algorithm, each agent requires a model of the grid to infer power imbalance, and that model may contain large errors. To assess the DGP algorithm's robustness to those errors, loads are given a linear model of the 39-bus system, and we examine the DGP algorithm's performance when a generator is disconnected from the system. This generator disconnection renders the model used by the loads as outdated and inaccurate, and simulation results indicate the DGP algorithm is robust to such model mismatch.

In principle, each agent in the DGP algorithm can be a consumer load. However, in this paper we assume that the

agents are aggregators, which are more suitable for providing contingency services in deregulated electricity markets since individual consumers are not well suited to take part in such markets [7]. Additionally, we assume the aggregators act on the transmission level directly. The balancing authority has a model of the transmission grid, which may then be supplied to the aggregators for use in the DGP algorithm. We do not consider the problem of computing actions for individual consumers within the aggregator (given the command to the aggregator). Methods such as those proposed in [4] can be used for making such decisions.

A. Literature review

The DGP algorithm was inspired by the work in [8], which also proposed a distributed algorithm to solve the same optimization problem: minimize total disutility subject to demand-supply being balanced. The key difference between the DGP algorithm and that in [8] (which we call the "dual" algorithm because it solves the dual problem) is that the dual algorithm is only applicable to strictly convex disutility functions, whereas the DGP algorithm is applicable to convex—but not necessarily strictly convex—disutility functions, i.e., disutility functions with affine regions. Not-strictly convex disutility is a more realistic model of consumers' disutility in response to demand variation because there may be no disutility for some small demand variation around the nominal demand but a positive disutility for variations higher than a threshold value, and such a model of consumer disutility is not strictly convex. For instance, it was shown in [9] that a small variation in fan power consumption of a commercial HVAC system led to no perceptible change in indoor climate, but a larger change in demand (from both the fan and the chiller) led to a $2\,\mathrm{deg\text{-}F}$ deviation from the set point. A strictly convex disutility cannot capture such a phenomenon because every demand variation—no matter how small—will have a nonzero cost.

A decentralized algorithm for controlling smart loads to provide contingency reserves was proposed in [10], and no grid model or communication is required; we call this algorithm the Optimal Load Control (OLC) algorithm. It was shown in [11] that the OLC algorithm performs well in the IEEE 39-bus system for small contingencies. However, the OLC algorithm also requires disutility functions that are strictly convex with respect to demand variation. Moreover, the analysis in [10] was deterministic, and it was shown in [12] that the OLC algorithm is vulnerable to mean-square instability in the presence of stochastic disturbance.

A core tenant of the DGP algorithm and those proposed in [8], [10] is that local frequency measurements provide global information about the state of the grid. The ability of loads to use local frequency measurements to infer global information was observed in [13], and frequency-based demand-side ancillary service has been a vibrant subject in the literature [14]–[17]. However, the approaches in these works only consider loads of the same type (e.g., smart refrigerators) and are not optimized to minimize disutility for heterogenous loads.

Another popular mechanism in the literature for loads to provide demand-side ancillary service is the use of price signals [18]–[20]. However, because contingencies are unplanned and must be mitigated in seconds (e.g., a generator trip), price signals will not be fast enough to provide on-line contingency service considered in this paper. Additionally, price signals are in units of price per energy, but change in demand is likely nonlinear—resulting in different prices for different changes in demand.

Another possible practice is the use of control signals distributed to loads by a central balancing authority [4], [9], [20]–[25]. However, centralized approaches either do not consider the disutility to consumers, or the central authority will require all problem data—including sensitive information such as demand and disutility—violating user privacy.

This paper is organized as follows. In Section II, we summarize the DGP algorithm. The use and identification of the grid model are described in Section II-C. In Section III, results of numerical studies are presented. Finally, Section IV presents conclusions of this work.

II. Summary of the DGP Algorithm

A. Problem Formulation

There are n loads (aggregators) in the power grid. Each load i may change its consumption by

$$x_i \in \Omega_i = [\underline{x}_i, \bar{x}_i].$$

There is a disutility function, $f_i(x_i)$, associated with load i's change in consumption. The generation in the grid is denoted as g, and the global difference between generation and consumption is denoted as $u = g - \mathbf{1}^T \boldsymbol{x}$, where $\boldsymbol{x}$ is the vector of x_i. It is the objective of the loads to change their consumption from their nominal values to obtain while minimizing their total collective disutility. Formally, the loads are to solve the following optimization problem:

$$\min_{x_i,\ i=1,\ldots,n} \sum_{i=1}^{n} f_i(x_i),\ \text{ s.t. } \sum_{i=1}^{n} x_i = g,\ x_i \in \Omega_i.$$

Each load i can obtain local noisy frequency measurements, $\Delta\tilde{\omega}_i$. Additionally, there exists a communication network among the loads, whose graph is denoted $\mathcal{G} = (\mathcal{V}, \mathcal{E})$, where the node set, $\mathcal{V} = \{1, 2, \ldots, n\}$, is the set of loads and the edge set, $\mathcal{E} \subseteq \mathcal{V} \times \mathcal{V}$, denotes the pairs of loads that can exchange information. The set of loads with whom load i can exchange information is denoted $\mathcal{N}_i = \{j | (i, j) \in \mathcal{E}\}$. This architecture is illustrated in Fig. 1.

B. The DGP Algorithm

The update law of the DGP algorithm consists of three main parts: i) a generation-matching step, ii) a gradient-descent step, and iii) a projection step. For the generation-matching step, each load uses its local frequency measurements and a model of the grid to infer and reduce the global power imbalance (see Section II-C); the power imbalance inferred by load i is

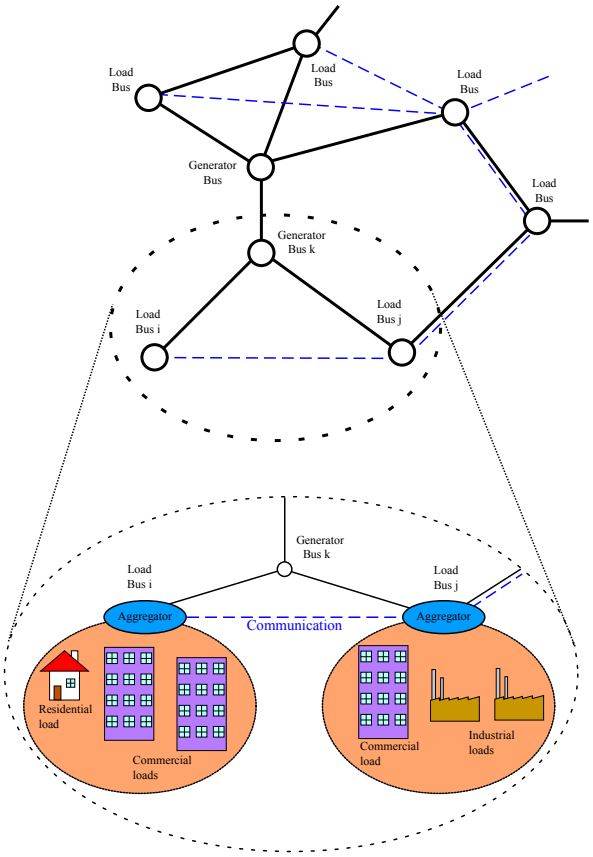

Fig. 1. Schema of DGP-algorithm architecture.

denoted $\hat{u}_i[k]$. The gradient-descent step utilizes load-to-load communication to equalize the loads' gradients. Finally, the projection step limits each load i's consumption change to its feasible range, .

The update law of the DGP algorithm for load i at time k is summarized in the following [5].

DGP Algorithm:

1) Obtain $\hat{u}_i[k]$ from the measurement $\Delta\tilde{\omega}_i[k]$ using a state estimator, which is described in Section II-C. The *generation-matching step* is then $\gamma[k]\hat{u}_i[k]$, where $\gamma[k]$ is a step size.
2) Compute gradient $\frac{d}{dx_i} f_i(x_i[k])$, transmit gradient value to neighbors, and receive neighbors' gradient values. Compute the *gradient descent step* $\Delta x_i[k]$ as the i^{th} entry of $\Delta\boldsymbol{x}[k]$, where
$$\Delta\boldsymbol{x}_k \triangleq -L\nabla f(\boldsymbol{x}_k)^T,$$
where L is the Laplacian matrix of the communication graph $\mathcal{G}$ [26].
3) Compute $x_i[k+1] = P_{\Omega_i}\big[x_i[k] + c\gamma[k]\Delta x_i[k] + \gamma[k]\hat{u}_i[k]\big]$, where $P_{\Omega_i}[\cdot]$ denotes the standard projection operator, $\gamma[k]$ is a step size, and c is a positive constant.

C. Estimating Global Power Imbalance

Each load uses its local frequency measurements and a linear, time-invariant (LTI) model of the grid to infer the global power imbalance using an algorithm proposed in [27], which estimates an unknown input from output measurements. This estimation is achieved by effectively "back-solving" the state-space equations for the input. In this application, the input to the model is power imbalance, and the output is power frequency. (For more details on the estimation algorithm, interested readers are referred to [8].) Therefore, each aggregator requires a discrete-time LTI model of the grid with power imbalance as the input and frequency deviation as the output. In practice, the balancing authority has a detailed model of the transmission grid, from which they can extract simplified models. These models in turn can be provided to aggregators.

For this work, each load needs a discrete-time LTI model of the IEEE 39-bus system. We use the least-squares identification method [28], in which unknown, discrete-time transfer-function parameters are estimated using input-output data from the 39-bus system. A pseudorandom-binary-sequence disturbance was applied to the 39-bus system, and a second-order transfer function was identified relating power imbalance to the mean frequency of the generators. Fig. 2 shows the step response of the identified model and the 39-bus system. This implementation of the 39-bus test system had the multi-band Power System Stabilizer (PSS) activated for system stabilization as implemented in [29]. It can be seen that the identified model is highly inaccurate due to the complexity of the 39-bus system and the simplicity of a second-order linear model.

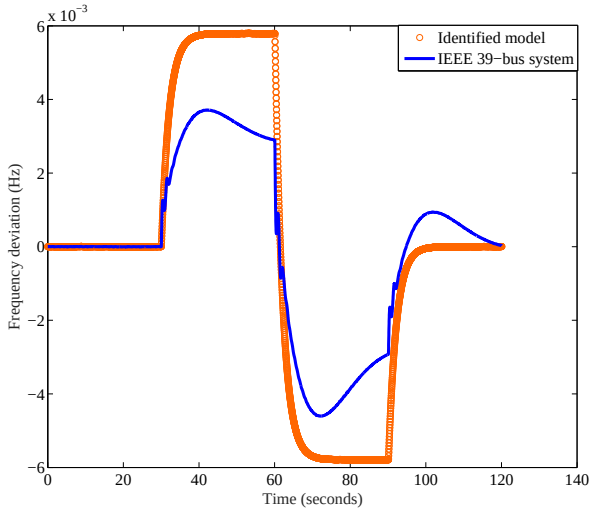

Fig. 2. Step response of identified LTI model and IEEE 39-bus system.

III. Results of Numerical Studies

A. Simulation Setup

The DGP algorithm was tested in the IEEE 39-bus test system, implemented in SimPowerSystems [29]. This system has 10 synchronous machines, each one of them with governor control and PSS. The test system has 19 loads, and each load

can modulate its consumption by $\pm 5\%$; that is, if the nominal consumption of load i is x_i^o, then $\Omega_i = [-0.05x_i^o, 0.05x_i^o]$.

We test the performance of the DGP algorithm with a convex (but not strictly convex) function:

$$f_i(x_i) = \begin{cases} 0, & |x_i| < a_i \\ \frac{1}{\beta_i}(x_i - a_i)^2, & x_i \geq a_i \\ \frac{1}{\beta_i}(x_i + a_i)^2, & x_i \leq -a_i \end{cases} \quad (1)$$

where $a_i = 0.05\bar{x}_i$ and β_i is chosen from a uniform distribution on $[0.1, 0.3]$ for each i. There is a communication delay for each load, i.e., each load only has access to past values of its neighbors' gradients. For frequency measurements, each load has access to the speed (frequency) of the closest generator, and those measurements are corrupted by zero-mean Gaussian noise with a standard deviation of 0.01% of the value of synchronous frequency (60 Hz), unless otherwise noted. The loads use the model identified in Section II-C to estimate power imbalance using the frequency measurements. It is considered that the consumption of loads vary over time. This fluctuation is modeled as Gaussian additive noise in power consumption of each load with zero-mean and standard deviation equal to 0.01% of the power of the load (except for Case study 5). The gains used in the DGP algorithm are $c = 5$ and $\gamma[k] = 0.06/(19 \max_i\{\beta_i\})$ for all k.

We conduct multiple case studies to assess: i) effect of model mismatch, ii) effect of communication delay, iii) effect of communication topology, iv) effect of measurement noise, and v) effect of uncertain, uncontrollable renewables. When one parameter is varied to study its effect, others are held constant at their nominal values. The nominal values for communication delay and measurement-noise standard deviation are 100 ms and 0.01%. The nominal edge set for the communication graph is $\mathcal{E} = \{(i,j) || i - j| = 1\}$.

B. Case 1: Model Mismatch and Communication Delay

To evaluate model mismatch, we disconnect generator 5 (508 MW) from the system at 5 seconds; generator 5 accounts for nearly 10% of the total generation in the system.

For communication delay, we use three different values for each scenario: no delay, 100 ms, and 1 second of communication latency between adjacent nodes. Fig. 3 shows the results of generator 5 being disconnected from the grid. Results for nominal operation (without smart loads) are shown for comparison. The frequency (speed deviation) shown is the mean deviation of all 10 generators from 60 Hz. Although the DGP algorithm only marginally aids in the voltage recovery at bus 20, the frequency deviation caused by the generator's disconnection is halved compared to the scenario without demand response. The DGP algorithm achieves this while using the original model identified in Section II-C, which is no longer accurate due to changes caused by the generator disconnection. In this case, the performance of the method is only marginally affected by the time delay in communications. The loss of a generator creates a much larger frequency deviation than the load increase in the following case studies. Therefore, the response of the DGP algorithm is dominated by the generation-matching term, which is not affected by communication delay.

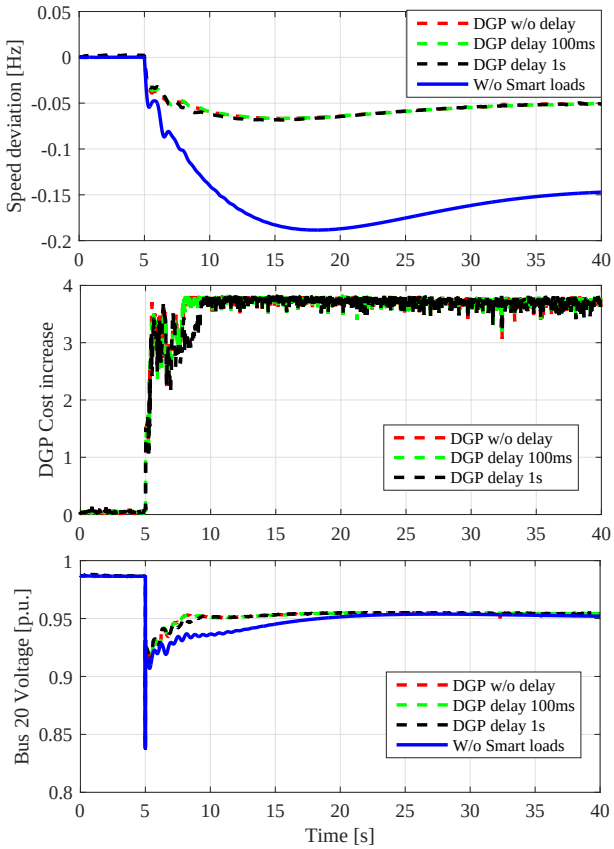

Fig. 3. Effects of model mismatch and communication delay: generator-5 disconnection.

C. Case 2: Load Increase and Communication Delay

Fig. 4 shows the results of a load disturbance applied to bus 27. Again, results without smart loads are shown for comparison. The DGP algorithm successfully arrests frequency deviations from the disturbance. In addition, the DGP algorithm halves the voltage drop at bus 27 caused by the disturbance compared to the scenario without demand response, and the voltage recovers more quickly under the DGP algorithm than nominal operation. These results are despite the inaccuracies in the identified model that the loads use to estimate the disturbance (see Fig. 2). Additionally, we can notice that a larger time delay in communications tends to worsen the response time of the DGP algorithm. In particular, the longer delay results in a longer time for the disutility to reach steady state. This is because the delay affects the gradient-descent step in the algorithm, which corresponds to minimizing disutility.

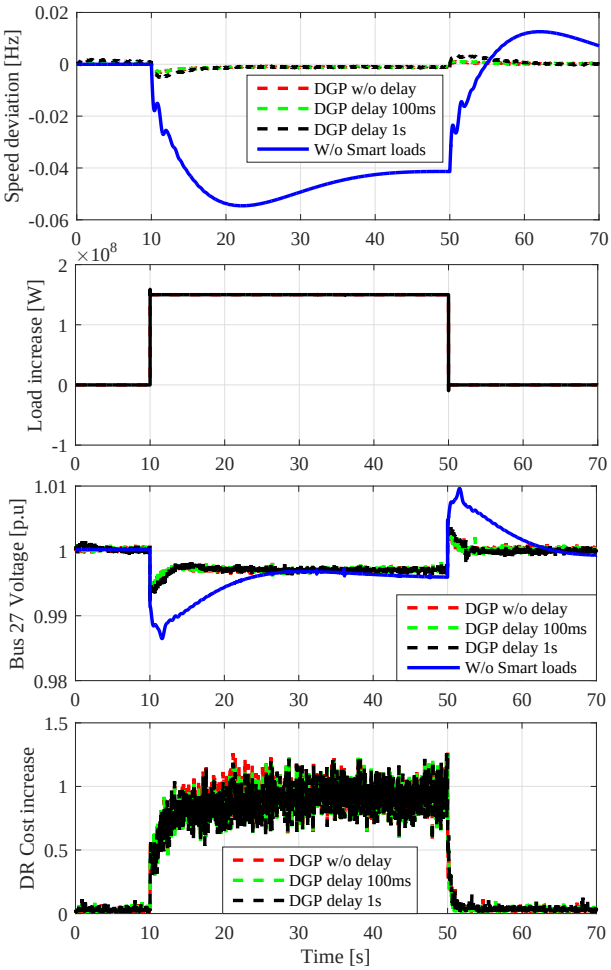

Fig. 4. Effect of communication delay: 150-MW load disturbance at bus 27.

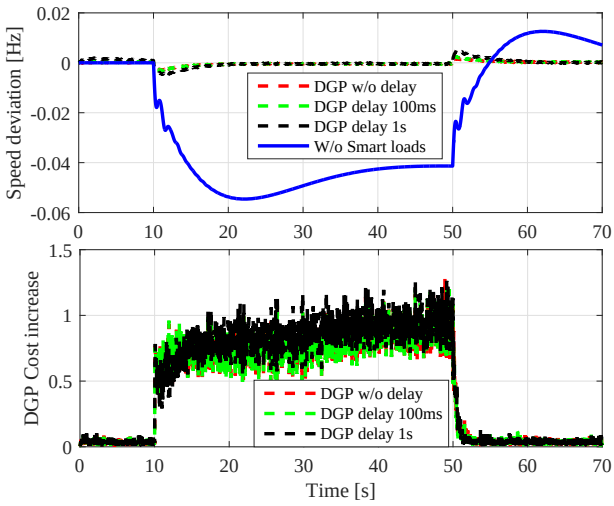

Fig. 5. Effects of change in topology and communication delay: 150-MW load disturbance at bus 27.

D. Case 3: Load Increase and Communication Topology

We have repeated the simulation of case study 2 changing the communication topology. The new edge set for the communication graph is given by $\mathcal{E}_2 = \{(1,2),(1,8),(1,13),(2,3),(3,4),(3,18),(4,19),(5,6),(6,7),(7,9),(7,10),(7,12),(7,15),(11,12),(13,14),(14,15),(14,17),(16,17)\}$, which is a connected graph that links the closest loads. Fig. 5 shows that changing the topology has little effect on the performance of the DGP algorithm.

E. Case 4: Load Increase and Measurement Noise

To evaluate the effect of frequency measurement noise, we have repeated the setup of case study 2 but fixing the communication time delay to 100 ms and setting the standard deviation of the frequency noise measurement to 0.01%, 0.1% and 1%. The results shown in Fig. 6 demonstrate that a noisy measurement can harm the performance of the DGP algorithm in terms of reducing frequency deviation. When compared to the performance of the system without smart loads, the results are superior for the cases where the standard deviation of noise is 0.01%, 0.1% and similar when it is equal to 1%. It is important to note that in the case without smart loads the control systems of the synchronous machines that keep the system stable do not rely on noisy measurements.

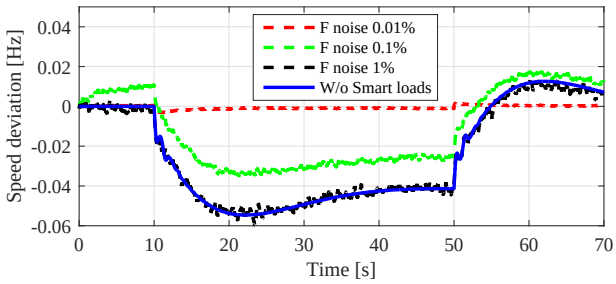

Fig. 6. Effect of noise in frequency measurement: 150-MW load disturbance at bus 27.

F. Case 5: Load Increase and Fluctuations from Renewables

The effect of widespread intermittent, uncertain, and uncontrollable renewable energy generation was considered as an increase in the fluctuation of the consumption from loads. This was modeled as an increase in the standard deviation of each load from 0.01% to 0.1% and 1% of the active power of the load. The same cases were also tested for the system without smart loads. This case used the same disturbance applied in case study 2 but with communication latency of 100 ms. The results depicted in Fig. 7 show that the DGP algorithm can compensate for the 10-fold increase in the uncertainty of load, but when the standard deviation of the noise is equal to 1%, the performance of the method is severely reduced. In comparison to the case without smart loads, however, there are gains with reduced speed deviation from the nominal value for all cases.

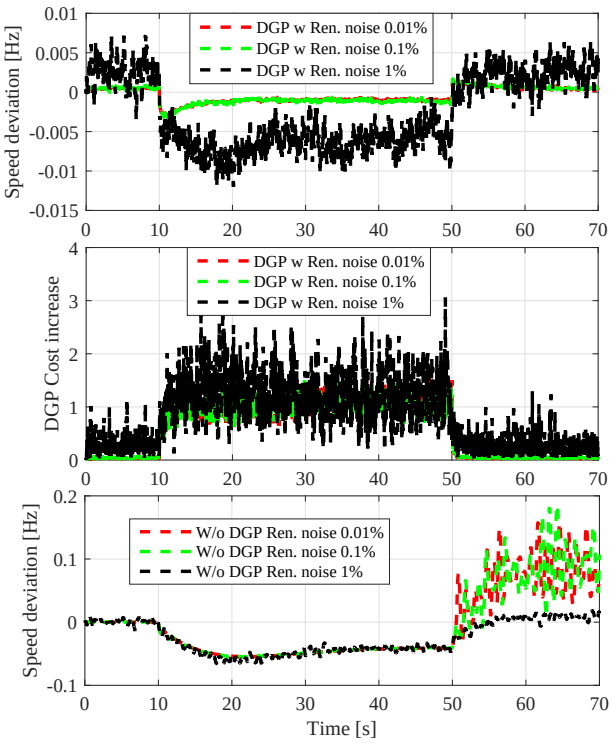

Fig. 7. Effect of fluctuations from renewable generation: 150-MW load disturbance at bus 27.

IV. Conclusion

The DGP algorithm proposed in [5] was designed for loads to provide contingency service in the power grid. The focus of this work was to evaluate the performance of the DGP algorithm in more-realistic scenarios than were considered in [5]. In the scenarios examined, the DGP algorithm was able to successfully arrest frequency deviations that result from a disturbance applied to the grid. The DGP algorithm requires each load to have a model of the grid, but numerical results suggest the DGP algorithm performs well even when the loads' model is inaccurate. It is the subject of future work to analyze other scenarios (e.g., change in topology of the power grid or a sensor with faulty measurements).

Acknowledgment

This work was supported by NSF grant CPS-1646229.

References

[1] B. Kirby, "Ancillary services: Technical and commercial insights," 2007, prepared for Wärtsilä North America Inc.

[2] F. Baccino, F. Conte, S. Massucco, F. Silvestro, and S. Grillo, "Frequency regulation by management of building cooling systems through model predictive control," in *18th Power Systems Computation Conference*, 2014.

[3] E. Vrettos, F. Oldewurtel, and G. Andersson, "Robust energy-constrained frequency reserves from aggregations of commercial buildings," *IEEE Transactions on Power Systems*.

[4] B. Biegel, L. Hansen, P. Andersen, and J. Stoustrup, "Primary control by ON/OFF demand-side devices," *IEEE Trans. on Smart Grid*, vol. 4, pp. 2061–2071, Dec 2013.

[5] J. Brooks and P. Barooah, "Consumer-aware load control to provide contingency reserves using frequency measurements and inter-load communication," in *American Control Conference*, July 2016, pp. 5008 – 5013.

[6] ——, "Distributed demand-side contingency-service provisioning while minimizing consumer disutility through local frequency measurements and inter-load communication," *arXiv preprint arXiv:1704.04586*, 2017.

[7] G. Barbose, C. Goldman, and B. Neenan, "A survey of utility experience with real time pricing," *Lawrence Berkeley National Laboratory*, 2004.

[8] C. Zhao, U. Topcu, and S. H. Low, "Optimal load control via frequency measurement and neighborhood area communication," *Power Systems, IEEE Transactions on*, pp. 3576–3587, 2013.

[9] Y. Lin, P. Barooah, S. Meyn, and T. Middelkoop, "Experimental evaluation of frequency regulation from commercial building HVAC systems," *IEEE Transactions on Smart Grid*, vol. 6, pp. 776 – 783, 2015.

[10] C. Zhao, U. Topcu, N. Li, and S. Low, "Design and stability of load-side primary frequency control in power systems," *IEEE Transactions on Automatic Control*, vol. 59, no. 5, pp. 1177–1189, 2014.

[11] I. Kamwa and A. Delavari, "Simulation-based investigation of optimal demand-side primary frequency regulation," in *Electrical and Computer Engineering (CCECE), 2016 IEEE Canadian Conference on*. IEEE, 2016, pp. 1–6.

[12] S. Pushpak and U. Vaidya, "Fragility of decentralized load-side frequency control in stochastic environment," *arXiv preprint arXiv:1702.03477*, 2017.

[13] F. Schweppe, R. Tabors, J. Kirtley, H. Outhred, F. Pickel, and A. Cox, "Homeostatic utility control," *IEEE Transactions on Power Apparatus and Systems*, vol. PAS-99, no. 3, pp. 1151 –1163, may 1980.

[14] J. A. Short, D. G. Infield, and L. L. Freris, "Stabilization of grid frequency through dynamic demand control," *Power Systems, IEEE Transactions on*, vol. 22, no. 3, pp. 1284–1293, 2007.

[15] P. J. Douglass, R. Garcia-Valle, P. Nyeng, J. Ostergaard, and M. Togeby, "Smart demand for frequency regulation: Experimental results," *Smart Grid, IEEE Transactions on*, vol. 4, no. 3, pp. 1713–1720, 2013.

[16] A. Molina-García, F. Bouffard, and D. S. Kirschen, "Decentralized demand-side contribution to primary frequency control," *Power Systems, IEEE Transactions on*, vol. 26, no. 1, pp. 411–419, 2011.

[17] S. H. Tindemans, V. Trovato, and G. Strbac, "Decentralized control of thermostatic loads for flexible demand response," *IEEE Transactions on Control Systems Technology*, vol. 23, no. 5, pp. 1685–1700, 2015.

[18] J. Mathieu, "Modeling, analysis, and control of demand response resources," Ph.D. dissertation, 2012.

[19] DoE, "Benefits of demand response in electricity markets and recommendations for achieving them," *US Dept. Energy, Washington, DC, USA, Tech. Rep*, 2006.

[20] P. Siano, "Demand response and smart grids: a survey," *Renewable and Sustainable Energy Reviews*, vol. 30, pp. 461–478, 2014.

[21] Y.-J. Kim, E. Fuentes, and L. K. Norford, "Experimental study of grid frequency regulation ancillary service of a variable speed heat pump," *IEEE Transactions on Power Systems*, vol. 31, no. 4, pp. 3090–3099, 2016.

[22] S. Meyn, P. Barooah, A. Bušić, Y. Chen, and J. Ehren, "Ancillary service to the grid from intelligent deferrable loads," *IEEE Transactions on Automatic Control*, vol. 60, pp. 2847 – 2862, March 2015.

[23] Monitoring Analytics, LLC, "State of the market report for PJM: Volume 2," Available online: http://www.monitoringanalytics.com/reports/PJM_State_of_the_Market/2015/2015-som-pjm-volume2.pdf, 2016.

[24] R. Walawalkar, S. Fernands, N. Thakur, and K. R. Chevva, "Evolution and current status of demand response (dr) in electricity markets: Insights from pjm and nyiso," *Energy*, vol. 35, no. 4, pp. 1553–1560, 2010.

[25] S. A. Pourmousavi and M. H. Nehrir, "Introducing dynamic demand response in the lfc model," *IEEE Transactions on Power Systems*, vol. 29, no. 4, pp. 1562–1572, 2014.

[26] C. Godsil and G. Royle, *Algebraic Graph Theory*, ser. Graduate Texts in Mathematics. Springer, 2001.

[27] P. K. Kitanidis, "Unbiased minimum-variance linear state estimation," *Automatica*, vol. 23, no. 6, pp. 775–778, 1987.

[28] K. J. Åström and P. Eykhoff, "System identificationa survey," *Automatica*, vol. 7, no. 2, pp. 123–162, 1971.

[29] A. Moeini, I. Kamwa, P. Brunelle, and G. Sybille, "Open data ieee test systems implemented in simpowersystems for education and research in power grid dynamics and control," in *Power Engineering Conference (UPEC), 2015 50th International Universities*. IEEE, 2015, pp. 1–6.